Online Characteristics Estimation of a Fuel Cell Stack through Covariance Intersection Data Fusion ⋆

Abolghasem Daeichian[a,*], Razieh Ghaderi[b], Mohsen Kandidayeni[b,c], Mehdi Soleymani[a], João P. Trovão[c], Loïc Boulon[b]

[a] *Department of Electrical Engineering, Faculty of Engineering, Arak University, Arak, 38156-8-8349, Iran*

[b] *Hydrogen Research Institute, Electrical and Computer Engineering Department, Université du Québec à Trois-Rivières, QC, Canada*

[c] *e-TESC lab, Department of Electrical and Computer Engineering, Université de Sherbrooke, QC, Canada*

Abstract

Employing semi-empirical models to estimate some characteristics of a fuel cell (FC) stack, such as power and polarization curves, is demanded for efficient design of a power allocation strategy in a FC hybrid electric vehicle. However, the multivariate nature of a FC system has made the design of an accurate model challenging. Since each semi-empirical model has its own pros and cons, this paper puts forward a data fusion approach for online characteristics estimation of a FC stack utilizing four well-known models, namely Mann, Squadrito, Amphlett, and Srinivasan. Despite the other similar techniques, the suggested one utilizes the strengths of each mentioned FC model while avoiding their drawbacks. Kalman filter is employed to identify the parameters of the models online to embrace the uncertainties caused by the alteration of operating conditions and degradation level. Considering the parameters, the output voltage given by each model as well as their covariance are computed. Then, a covariance intersection algorithm is proposed to fuse the estimated output voltages. The fusion of the models' outputs leads to the estimation of fused characteristics curves. To underline the effectiveness of the proposed method, it is applied to four different experimental datasets extracted from three 500-W Horizon FCs. The obtained results demonstrate the superior performance of the suggested estimator in the sense of mean square error. On average, the mean square error of the data fusion method is 39.64% and 36.59% lower than other studied methods while estimating the polarization curve and power curve, respectively.

Keywords: Data fusion, Energy management strategy, Modeling, Online identification, Proton exchange membrane fuel cell

1. Introduction

1.1. Motivation

Transportation division is one of the main causes of human-induced greenhouse gas emissions worldwide owing to its dependency on fossil fuels. To deal with this issue, the use of electrified vehicles through the development of hybrid electric vehicles (HEVs) and pure electric vehicles have received great attentions [1]. Nevertheless, the reliance of HEVs on fossil fuels and the long recharging time of batteries have provided the basis for the appearance of other technologies like

proton exchange membrane (PEM) fuel cells (FCs) in this domain [2]. Compared to other kinds of FC, PEMFC benefits from higher power density and lower temperature and pressure operating ranges. While a PEMFC has these distinct virtues, it cannot meet all the requisites for supplying a vehicular power demand owing to its incapacity to store energy, slow dynamic response, and so forth. Hence, it is normally hybridized with a buffer, like a battery or supercapacitor, to compensate for the mentioned weaknesses. Since the intrinsic characteristics of the PEMFC and buffers are different, a power allocation strategy (PAS) is necessary to dispense the power between the sources in a way to minimize the hydrogen consumption and maximize the lifetime and efficiency of the system [3]. Several PASs have hitherto been introduced for FC hybrid electric vehicles (FCHEVs) that can be grouped into three categories of rule-based, optimization-based and intelligent-based [4, 5]. Most of these strategies are based on PEMFC models designated by static characteristics maps (power, efficiency, voltage, etc.) to ascertain the FC voltage/power as the main power source in a FCHEV. However, several papers have reported the impact of ambient and/or operating conditions variation (current, temperature, humidity, etc.) and ageing on the performance of the PEMFC. For instance, in [6], the degradation of the PEMFC is studied after 20 times freezing and thaw cycles using different electrochemical tests. In [7], the influence of operating temperature on the current density distribution and membrane resistance is studied and concluded that the increase of load leads to the inhomogeneity of the current density distribution. In [8], it is demonstrated that air relative humidity has a noticeable impact on the PEMFC performance while the hydrogen humidity has almost no effect. The study conducted in [9] illustrates that the classical PASs confronts mismanagement problems when the PEMFC characteristics vary because of the discussed reasons.

1.2. Literature review

In the light of the described issues, some solutions have been proposed to enhance the performance of a PAS while facing the uncertainties in the PEMFC stack.

The first one is to integrate a FC degradation model into formulation of the PAS. It has been practiced in several studies. In [10], the degraded FC is modeled based on polarization curve and power distribution is tuned adaptively during the whole lifetime of the stack. In [11], an attention mechanism is combined with recurrent neural network to perform an accurate prediction of the output voltage degradation of PEMFC. While these methods can improve the performance of a PAS to a certain level, they do not consider the variation of characteristics owing to the ambient conditions. Moreover, the FC degradation phenomenon is an intricate mechanism and its modeling regarding the operating conditions of a FCHEV is still an ongoing problem. The second approach to deal with the uncertainties of the FC system is the inclusion of an extremum seeking algorithm (ESA) in the PAS development [12, 13]. A fractional-order based ESA is proposed in [12] to search for the extremum value of a static nonlinear curve. It utilizes a gradient based optimization process by imposing a periodic perturbation signal to the input of the system and then changing it towards the maximum/minimum point. Another ESA based on bidimensional optimization, taking the hydrogen consumption and PEMFC system power into account, is suggested in [13]. Such ESAs are of interest due to their simplicity of integration into a PAS formulation. Nevertheless, the complication of these algorithms increases when the identification of several operating points is required. Indeed, this is the case in a PAS application where several characteristics are sought after at the same time.

To evade the above-mentioned matters, the use of parameter estimation methods has been proposed in the PAS formulation of a FCHEV [14]. In this respect, a FC semi-empirical (grey-box) model is utilized to provide the required characteristics for a PAS while the parameters of the

model are updated from time to time. Modeling and parameter estimation go hand in hand indeed. In [15], six semi-empirical models, proposed by Srinivasan et al., Kim et al., Lee et al., Mann et al., Squadrito et al., and Kulikovsky et al., are introduced. Among them, the one put forward by Squadrito et al. is selected based on the number of required measurement sensors and the considered physical phenomena. Moreover, its parameters are estimated by recursive least squares (RLS) method. In [16], three semi-empirical models, namely Squadrito, Amphlett, and Boulon, are compared for the automotive cold startup application while using recursive maximum likelihood (RML) as the estimator, and Amphlett's model is selected as the most accurate one. In [17], Squadrito and Amphlett models are compared for the PAS application while utilizing three parameter estimators (Kalman filter (KF), RLS, and extended KF). The authors show that Amphlett is more suitable for online characteristics extraction, and KF and extended KF perform marginally better than RLS in terms of precision. In [18], the efficiency-vs.-power curve of the FC stack is estimated by means of a third-order polynomial function where its parameters are identified online by RLS. In [19], another polynomial model is proposed to estimate the hydrogen consumption of the FC stack using RLS. In [20], a supervisory PAS is formulated where a current-dependent model coupled with RLS is used for the FC system. Ettihir et al. have used square root unscented KF for parameters estimation of the model introduced by Squadrito et al. and included it into the formulation of a hysteresis and an optimal PAS [21]. In [22], the robustness of two methods, namely RLS and RML, are studied while facing additional noise in the system. It is concluded that RML has a marginally better performance in the presence of noise. In [23], a learning method for the estimation of the unknown measurement noise while identifying the parameters of a PEMFC model is proposed. In [24], an adaptive parameter estimator based on Lyapunov method is suggested to estimate four parameters of a FC model. While the exponential convergence of this method is shown, its asymptotic stability is not guaranteed.

1.3. Contribution and organization

With respect to the above-discussed papers, it can be stated that different semi-empirical models have different characteristics, capabilities, and levels of trust. For instance, some models consider stack temperature while others consider partial pressure of oxygen. Moreover, some models only focus on specific regions of a polarization curve while others represent the whole curve. For this reason, having a model of PEMFC that can combine all the advantages of the mentioned models may result in better estimation of PEMFC characteristics. In this regard, this paper proposes a data fusion technique based on covariance intersection (CI) to synthesize the merits of four well-known semi-empirical models in the literature. To the best of the authors' knowledge, this is one of the first attempts if any, to fuse the output of several PEMFC semi-empirical models for extracting the required characteristics in a PAS design application. To this end, a CI data fusion algorithm has been employed. In the proposed algorithm, the parameters of Squadrito, Amphlett, Srinivasan and Mann models are identified by KF, which is known as a reliable estimator in the literature. Then, the predicted output voltage and its covariance are calculated for each model. Finally, the data are fused by the CI. The proposed method has been tested using four different datasets (DSs) obtained from a developed experimental setup. The obtained results show that on one hand the estimated voltage is as precise as the best estimations of the models. On the other hand, the fused estimation is more reliable than that of each model due to reducing the covariance estimation.

The remainder of this paper is organized as follows: the PEMFC semi-empirical models are introduced in section 2. The parameter identification algorithm is represented in section 3. The proposed covariance intersection algorithm is discussed in section 4. Section 5 is devoted to the simulation and experimental results. At last, the paper is concluded in section 6.

2. Models of PEMFC

Several semi-empirical models are introduced for PEMFCs in the literature. In this paper, four models have been selected whose structures lead to regressor linear-in-parameter equations in the sense of parameter identification. A linear regression equation has been defined for each model as $V_{FC} = \sum_{i=1}^{n_\theta} \theta_i x_i$, where θ_i is the unknown parameters of the model and x_i is the known values (regressors). Assuming $\theta^T = [\theta_1, \dots, \theta_{n_\theta}]$ and $X^T = [x_1, \dots, x_n]$ leads to $V_{FC} = X^T\theta$ where ^{T} denotes the transpose of a vector. Below, the four considered PEMFC models and the related unknown parameters and regressors are presented. The goal of parameter identification is to estimate the unknown parameters θ for each model so that the sum squared error with respect to data samples $\{v_{FC}(t), i_{FC}(t), T_{FC}(t)\}$ is minimized.

2.1. Mann et al. model

Mann et al. [25] have modeled the cell potential V_{FC} as the summation of the ohmic over-voltage η_{ohm}, the activation over-voltage η_{act}, and the Nernst potential E_{nernst}:

$$V_{FC} = E_{nernst} + \eta_{act} + \eta_{ohm} \tag{1}$$

The thermodynamic potential of the chemical reaction inside the PEMFC is called the Nernst potential which relies on the PEMFC temperature T_{FC} and the partial pressure of oxygen and hydrogen, P_{H_2} and P_{O_2} as:

$$E_{nernst} = 1.229 - 0.85e^{-5}(T_{FC} - 298.15) + 4.308e^{-5}T_{FC}\left(\log\left(P_{H_2}\right) + 0.5\log\left(P_{O_2}\right)\right) \tag{2}$$

The summation of the anode and cathode over-voltage determines the activation over potential η_{act}. It depends on the cell characteristics as:

$$\eta_{act} = \xi_1 + \xi_2 T_{FC} + \xi_3 T_{FC}\log\left(C_{O_2}\right) + \xi_4 T_{FC}\log(i_{FC}) \tag{3}$$

where the unknown parameters $\xi_i, i = 1, 2, 3, 4$ are experimental parameters depending on the kinetics of the reaction. Finally, the internal resistance $r_{internal}$ specifies the ohmic over-voltage:

$$\eta_{ohm} = -i_{FC} r_{internal} \tag{4}$$

where

$$r_{internal} = \mu_1 + \mu_2 T_{FC} + \mu_3 i_{FC} + \mu_4 T_{FC} i_{FC} + \mu_5 T_{FC}^2 + \mu_6 i_{FC}^2 \tag{5}$$

Putting equations (1) to (5) together results in the regression equation as

$$V_{FC} - E_{nernst} = X^T\theta \tag{6}$$

where

$$\theta^T = [\xi_1, \xi_2, \xi_3, \xi_4, \mu_1, \mu_2, \mu_3, \mu_4, \mu_5, \mu_6]$$
$$X^T = [1, T_{FC}, i_{FC}, T_{FC}i_{FC}, T_{FC}^2, i_{FC}^2, -i_{FC}, -i_{FC}T_{FC}, -T_{FC}i_{FC}^2, -i_{FC}T_{FC}^2, -i_{FC}^3]$$

2.2. Squadrito et al. model

The output voltage of FC in the model proposed by Squadrito et al. [26] relies on the open-circuit voltage V_0, the current of the FC i_{FC} and the FC ohmic resistance r as follows:

$$V_{FC} = V_0 - b\log(i_{FC}) - r i_{FC} + \alpha i_{FC}^k \log(1 - \beta i_{FC}) \tag{7}$$

where α and k are fitting parameters, and k is a constant between $[1, 4]$. Here, the measured values are V_{FC} and i_{FC} while $\{V_0, r, \alpha, k\}$ are unknown parameters. As a result, in the sense of identification we have:

$$\theta^T = [V_0, b, r, \alpha]$$
$$X^T = \left[1, -\log(i_{FC}), -i_{FC}, i_{FC}^k \log(1 - \beta i_{FC})\right]$$

where x_i and θ_i are regressors and regression coefficient (parameter) vectors, respectively. It is worth noting that the mass transport over potential is a benefit of Squadrito model. However, the temperature dependence of the output voltage is not considered.

2.3. Amphlett et al. model

Amphlett et all [27] represent a general formulation of electrochemical PEMFC. This model is not only applicable in the situation of series connection of several FCs but also different operating conditions are taken into account as it could be seen in (8). In addition, because of its structure in the concentration loss calculation, this model creates a great opportunity to compare the impact of linear and nonlinear parameter identification.

$$\begin{aligned} V_{FC} &= N(E_{nernst} + V_{act} + V_{ohmic} + V_{con}) \\ V_{act} &= \xi_1 + \xi_2 T + \xi_3 T \ln(C_{O_2}) + \xi_4 T \ln(i_{FC}) \\ C_{O_2} &= \frac{P_{O_2}}{5.08\times10^6 \exp\left(-\frac{498}{T}\right)} \\ V_{ohmic} &= -i_{FC} R_{internal} = -i_{FC}(\mu_1 + \mu_2 T + \mu_3 i_{FC}) \\ V_{con} &= B \ln\left(1 - \frac{J}{J_{max}}\right) \end{aligned} \quad (8)$$

where V_{FC}, V_{act}, V_{ohmic}, V_{con} are the output, activation loss, ohmic loss, and concentration loss voltage, respectively. The stack temperature (K) is denoted by T. P_{H_2} and P_{O_2} denote the hydrogen partial pressure in the anode side (Nm^{-2}) and the oxygen partial pressure in the cathode side (Nm^{-2}). ξ_n, $(n = 1, \dots, 4)$ are the semi-empirical coefficients based on thermodynamics, fluid mechanics, and electro chemistry. C_{O_2} is the oxygen concentration $molcm^{-3}$. Moreover, $R_{internal}$, i, J, J_{max}, and B indicate the internal resistor (Ω), PEMFC operating current (A), actual current density (Acm^{-2}), maximum current density (Acm^{-2}), and a parametric coefficient (V), respectively. Finally, μ_n, $(n = 1, \dots, 3)$ are parametric coefficients. The set of unknown parameters and regressors could be considered as:

$$\theta^T = [\xi_1, \xi_2, \xi_3, \xi_4, \mu_1, \mu_2, \mu_3, B]$$
$$X^T = \left[1, T, T\ln(C_{O_2}), T\ln(i_{FC}), -i_{FC}, -i_{FC}T, -i_{FC}^2, \ln\left(1 - \frac{J}{J_{max}}\right)\right]$$

2.4. Srinivasan et al. model

Srinivasan et al. model [28], founded on experimental data, can be defined as:

$$V_{cell} = V_0 - b\log(i_{FC}) - r i_{FC} \quad (9)$$

$$V_0 = V_r + 2.303\frac{RT_{FC}}{\xi}\log(i_{FC}) \quad (10)$$

where r, b, i_0, ξ, V_r denote the slope of the linear region with nonlinear least square fits, the Tafel slope, the exchange current, the transfer coefficient of the oxygen reduction, and the reversible potential for the cell, respectively. Since calculating V_0 by (10) requires some information from the FC stack, which is not easily accessible, this parameter is considered unknown and estimated by the developed methods. So,

$$\theta^T = [V_0, b, r]$$

$$X^T = [1, -\log(i_{FC}), -i_{FC}]$$

This model has been used frequently in the literature due to its simplicity. The main drawback of this model is that it neglects the mass transport overvoltage. Furthermore, the influence of temperature on the output voltage is not considered in this model.

The main characteristics of the aforementioned models are listed in Table 1.

Table 1: Comparison of models

Model	Mass transport	Temperature	No. of Parameters
Mann	No	Yes	10
Squadrito	Yes	No	4
Amphlett	Yes	Yes	8
Srinivasan	No	No	3

3. Parameter Identification Algorithm

Online parameter identification has been performed by numerous algorithms. One of the most well-known and widely used algorithms is KF. It consists of predicting one-step ahead of the state variables and updating the predicted value with the new measurement. Assuming the actual state and measurement model as:

$$\begin{aligned} \theta(t+1) &= F_t\theta(t) + B_t u(t) + w(t) \\ y(t) &= H_t\theta(t) + n(t) \end{aligned} \tag{11}$$

where y, u, and θ denote measurements, control-inputs, and states, respectively. The matrix F_t, B_t, and H_t are state, input, and observations matrix. w and n are zero-mean and normally distributed noises with covariance W_t and R_t, respectively, which contaminate the process and measurements. Two alternate phases of the KF are the prediction phase as:

$$\begin{aligned} \hat{\theta}(t|t-1) &= F_t\hat{\theta}(t-1|t-1) + B_t u(t-1) \\ P(t|t-1) &= F_t P(t-1|t-1)F_t^T + W_t \end{aligned} \tag{12}$$

where $\hat{\theta}(t|t-1)$ and $P(t|t-1)$ are a priori state estimate and a priori estimate covariance, respectively, and the update phase as:

$$\begin{aligned} \hat{\theta}(t|t) &= \hat{\theta}(t|t-1) + K(t)\left(y(t) - H_t\hat{\theta}(t|t-1)\right) \\ P(t|t) &= (I - K(t)H_t)P(t|t-1) \\ K(t) &= P(t|t-1)H_t^T(H_t P(t|t-1)H_t^T + R_t)^{-1} \end{aligned} \tag{13}$$

where $\theta(t|t)$, $P(t|t)$, and $K(t)$ are a posteriori state estimate, a posteriori estimate covariance, and Kalman gain, respectively.

The KF, which has its reputation due to optimally estimating the state of systems, can be utilized as a parameter estimator to extract the interesting parameters from the noisy measurements. The parameter estimation problem can be adopted to state-space framework as:

$$\begin{aligned} \theta(t+1) &= \theta(t) + w(t) \\ y(t) &= X_t^T\theta(t) + n(t) \end{aligned} \tag{14}$$

where the states are unknown parameters θ which need to be estimated. The output is considered to be the measured values y and the output matrix is the regressors X_t. $w(t)$ and $n(t)$ are assumed to be parameters and measurement noise with covariance matrices W and R, respectively.

Assuming independent parameters, a diagonal covariance matrix are typically chosen. W represents not only the strength of the time variance of parameters but also gives the capability to determine the forgetting factor for each parameter individually. This capability of KF outperforms the RLS. $W = 0$ is equivalent to forgetting factor equal to one in RLS. Substituting the model (14) into the KF algorithm, the prediction phase vanishes and we have:

$$\begin{aligned} &\hat{\theta}(t) = \hat{\theta}(t-1) + K(t)\left(y(t) - X_t^T\hat{\theta}(t-1)\right) \\ &K(t) = (X_t^T P(t-1) X_t + R_t)^{-1} P(t-1) X_t \\ &P(t) = (I - K(t)X_t^T)(P(t-1) + W) \end{aligned} \tag{15}$$

The noise covariance R is commonly considered as a constant.

4. Data Fusion

The process of merging multiple data to produce more accurate and consistent information than provided by any individual data source is called data fusion. According to the joint directors of laboratories (JDL) model, data fusion could be performed in the level of data, sensor, and information [29]. One of the most popular methods of data fusion is based on covariance intersection (CI) algorithm that takes convex combination of mean and covariance of estimations. CI is naturally endowed with some properties, such as being distributed and decentralized, which offer the possibility of plug-and-play data fusion [29, 30]. CI presents a sub-optimal data fusion algorithm avoiding the assumption of estimates independence required by standard Bayesian filters. CI merges the estimates of different sources by weighing and using a mixing parameter. The mixing parameters are usually found through an optimization, such as minimizing the trace (or determinant) of the fused covariance matrix [30]. It is equivalent to minimizing the Shannon entropy of the fused covariance matrix. This paper mainly concerns providing a better estimation for the PEMFC characteristics and output voltage utilizing four semi-empirical models. Employing KF and considering any semi-empirical models that was discussed in section 2, the output voltage of the FC could be estimated. The more accurate any estimation be the more weight will be given to the CI data fusion. Each semi-empirical model may provide the best estimation in a specific working situation of FC. The CI follows the best estimation in each time step and in different situations. The CI not only attempts to reduce the mean square error (MSE) but also reduces the covariance of estimation. Therefore, not only having more accurate models but also having more precise estimation can lead to better results.

The CI fuses $i = 1, \dots, n$ data with mean V_i and covariance P_i as:

$$P_{DF}^{-1} = \sum_{i=1}^{n} \omega_i P_i^{-1} \tag{16}$$

$$P_{DF}^{-1} V_{DF} = \sum_{i=1}^{n} \omega_i P_i^{-1} V_i \tag{17}$$

where the weights ω_i are chosen in a way to minimize the trace of P_{DF}. In this paper, the regression vector of each semi-empirical model, defined in section 2, is calculated by using the observations i_{FC} and T_{FC}. Then, KF identifies the parameters of the model $i = 1, \dots, n$ and determines $\hat{\theta}_i$ and covariance of the estimated parameters P_i. An estimation for the output voltage could be obtained by substituting the estimated parameters into the related model. It is easy to show that the covariance of the estimated output voltage is:

$$\mathbb{P}_i = X_i^T P_i X_i + R_i \tag{18}$$

P_i is affected by the number of parameters of the model. So, the CI algorithm is modified to remove the effect of the number of parameters on the estimated output voltage as follows:

$$P_{DF}^{-1} = \sum_{i=1}^{n} \omega_i \frac{1}{n_{\theta_i}^2} \mathbb{P}_i^{-1} \tag{19}$$

$$V_{DF} = P_{DF} \sum_{i=1}^{n} \omega_i \frac{1}{n_{\theta_i}^2} \mathbb{P}_i^{-1} V_i \tag{20}$$

where n_{θ_i} is the number of parameters i and ω_i is obtained by solving an optimizing problem with the following cost function:

$$\omega_i = \min_{\omega_i} \left[\text{trace} \sum \frac{\omega_i}{n_{\theta_i}^2} \mathbb{P}_i^{-1} \right] \tag{21}$$

The presented algorithm is depicted in Fig. 1.

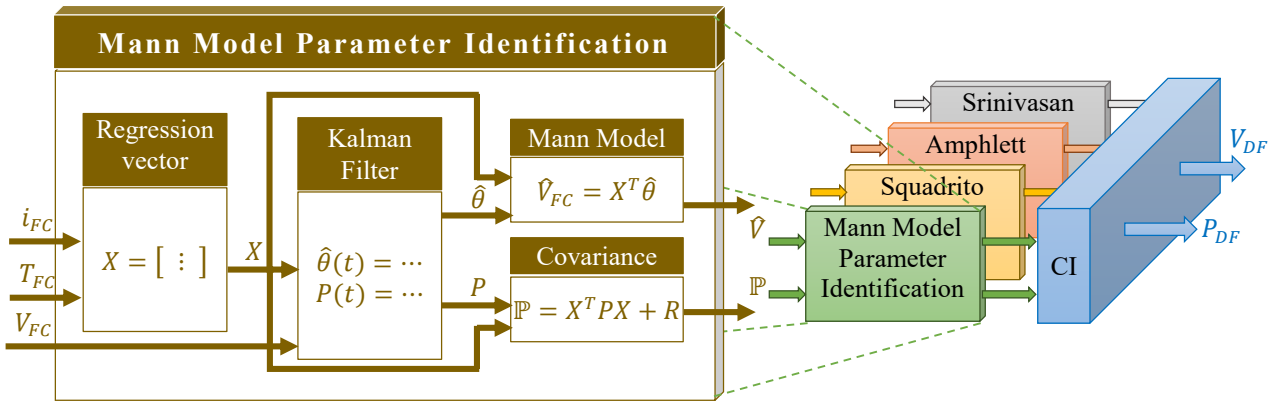

Figure 1: Structure of the suggested estimation process based on data fusion.

5. Results and Discussion

5.1. Experimental set-up

To validate the performance of the suggested estimator based on data fusion, an experimental set-up has been utilized for data collection. Fig. 2 demonstrates this set-up where a Horizon H-500 PEMFC is connected to some measurement instrumentations for testing the estimation process. This air-cooled PEMFC is equipped with two axial fans to provide the oxygen on the cathode side and cool down the stack. The maximum stack temperature is 65℃. Typically, open cathode FCs are known to have a lower operating stack temperature compared to the closed cathode ones [31, 32]. Moreover, this FC is self-humidified and operates based on a dead-ended anode (DEA) configuration in which the dry hydrogen is regularly supplied at a particular inlet pressure. A hydrogen supply valve is utilized in the anode inlet to deliver dry hydrogen to the PEMFC, having a flow rate from 0 to 7 l/min with respect to the drawn current. The anode outlet has a purge valve to expel the buildup of water and nitrogen out of anode volume and replenish it with fresh hydrogen. The purge valve is normally closed and does a cyclic purging every 10 s for a duration of 100 ms while the PEMFC is under operation. A manual forward pressure regulator, as shown in Fig. 2, is used to maintain the hydrogen partial pressure between 0.45 and 0.6 bar. The pressure difference between the anode and cathode sides must not exceed 0.5 bar to decrease the membrane damage. Mass flowmeter and a hydrogen tank are the other hydrogen supply subsystems of this FC stack.

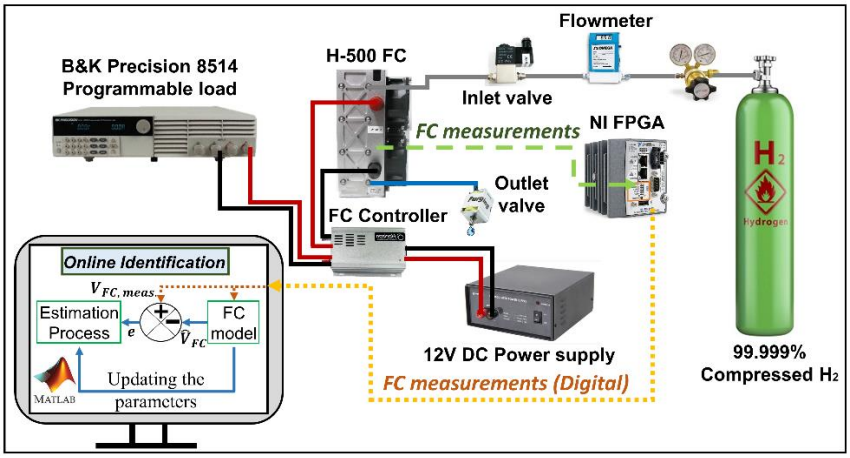

Figure 2: Experimental set-up

From Fig. 2, the utilized PEMFC stack is connected to a Natural Instrument CompactRIO (NI cRIO-9022) through its controller. The fans as well as the inlet/outlet valves are controlled by the control unit of the PEMFC. The communication between cRIO and PC is accomplished by an Ethernet connection where current, temperature, and voltage are recorded with a sampling frequency of 10 Hz. These measured data are utilized for performing the online estimation process in Matlab software which is available in the PC. A DC Electronic Load (8514 BK Precision) is utilized to draw a load profile from the FC stack.

For the validation purpose of this work, four different DSs including current, voltage, and temperature, are utilized with four different initial ambient temperatures. These four DSs have been obtained from three Horizon H-500 FCs with different degradation levels. Since the utilized FCs have different ageing milestones and have been produced in different years, they have various characteristics in terms of power and voltage delivery. To determine the ageing extent of each FC, their voltage-vs.-current (polarization) and power-vs.-current curves are illustrated in Fig. 3 as an indicator of their actual health state. To obtain the polarization curve of each stack, a fixed current has been applied to the FC and its output voltage value has been recorded after 15 minutes for each rising current level. From Fig. 3, it can be observed that two polarization tests have been done on the FC1. One test has been done at ambient temperature of 21℃ ($FC1: Ref._{DS1}$), and one test has been carried out at ambient temperature of 28℃ ($FC1: Ref._{DS3}$). From these two tests, it can be stated that FC1 has reached a maximum power of around 405 W and 384 W in case of $Ref._{DS1}$ and $Ref._{DS3}$ tests, respectively. This variation of maximum power is due to the difference in ambient conditions. Regarding FC2, it can be seen from $FC2: Ref._{DS2}$ that this FC is in a better health state as it can reach a maximum power value of almost 455 W. This test has been performed at ambient temperature of 24℃. $FC3: Ref._{DS4}$ demonstrates the polarization and power curves of FC3at ambient temperature of 23℃. It can be seen that this FC can deliver the highest maximum power (around 600 W) among the tested FCs. Regarding FC1 and FC2, the polarization tests have been continued until the voltage drop due to concentration at high current region is observed. However, concerning FC3, the test has been stopped at 40 A in order not to damage the FC system. According to the manufacturer, the shut-down current limit for this FC is 42 A.

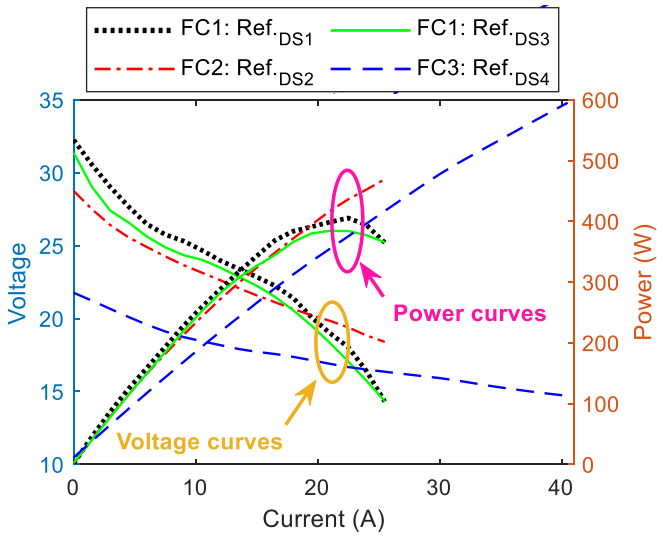

Figure 3: Experimental polarization and power curves.

The acquired polarization and power curves will be used to validate the characteristics estimation of the proposed method. The technical specifications of the utilized PEMFCs in this manuscript are presented in Table 2. The technical data of FC1 and FC2 have been collected from [33] and the technical data of FC3 are available in [34], which are the provided manuals of the employed FCs by the manufacturer.

Table 2: Specifications of the used Horizon H-500 PEMFCs

Technical Data	Utilized FC	
	FC1 and FC2	FC3
Type	Open cathode	Open cathode
Number of cells	36	24
Hydrogen pressure	0.5-0.6 Bar	0.45-0.55 Bar
Cathode pressure	1 Bar	1 Bar
Ambient temperature	5-30 $°C$	5-30 $°C$
Maximum stack temperature	65 $°C$	65 $°C$
Hydrogen purity	99.999% dry H2	≥ 99.995% dry H2
Size	130 × 220 × 122 (mm)	130 × 268 × 122.5 (mm)
Cooling	Air (integrated cooling fan)	Air (integrated cooling fan)

Fig. 4 presents the current and measured stack temperature of the employed DSs. Figs. 4a and 4c show the DS1 and DS3 current profiles, respectively, which are applied to FC1. DS1 is a random current profile fluctuating almost within the whole operating current of FC1 at ambient temperature of 21℃. DS3 has been obtained by means of the Urban Dynamometer Driving Schedule (UDDS) which characterizes the driving condition in a city. In this respect, the UDDS driving cycle has been used as the input of IEEE VTS Motor Vehicles Challenge in [35], and the subsequent demanded current from the FC system has been scaled within the operating range of FC1. As this current profile comes from a driving cycle, it can replicate a real situation that may occur to a FC system in a vehicular application. Fig. 4b illustrates the requested current from FC2 (DS2), which is a rising step current profile within the operating range of FC2 at ambient temperature of 24℃. Fig. 4d shows the applied current to FC3 (DS4) at ambient temperature of

23℃. It is also a step-up current profile with longer step durations compared to DS2. It should be reminded that the main idea behind using different DSs and FCs is to impose the estimators to various excitation signals and FC technologies and then study the accuracy of the proposed estimators accordingly. Indeed, the variation in the conditions of data collection is interesting as it can influence the output voltage and power of the PEMFCs and make the characteristic estimation problem more challenging for the proposed data fusion based estimator. One worth noting point about Fig. 4 is that it shows the current and temperature of the FC are interdependent. This interdependency makes the estimation process challenging as most estimators have been developed for systems with independent variables. Although FC current and temperature are dependent, the dynamic of temperature is much slower than current. Since the measurements are received every 100 ms in this work, it is assumed that temperature is constant during each time step. Therefore, the measured signals are sent to the estimators at each time step, and they then identify the parameters of the model before the next measurement arrives. Table 3 provides more information on the utilized experimental data. According to Table3, DS1 has the longest duration with 32821 samples which takes around 55 minutes. The measured voltage along with the estimated ones are discussed in the next section.

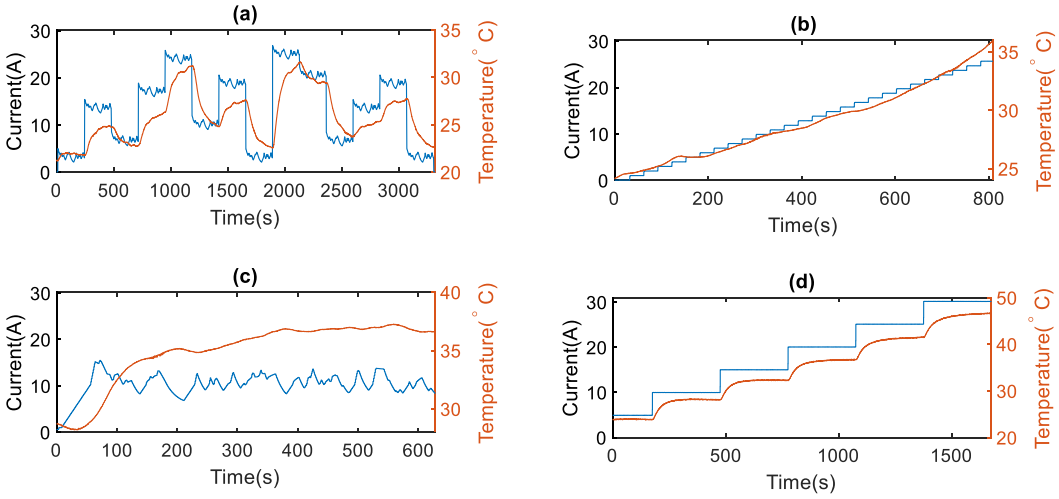

Figure 4: Experimental DSs, a) DS1 (FC1), b) DS2 (FC2), c) DS3 (FC1), and d) DS4 (FC3)

Table 3: The collected DSs

DS No.	No. of samples	Ambient condition		Used FC
		Temperature (°C)	Humidity (%)	
DS1	32821	21	60	FC1
DS2	8000	24	65	FC2
DS3	6220	28	63	FC1
DS4	16585	23	67	FC3

5.2. Results analysis

To validate the performance of the proposed estimation method, three analyses are performed in this section. Firstly, the online estimation of the PEMFC output voltage is compared with the measured one for each of the utilized models. This is a general consideration regarding the estimation process. Subsequently, the variance of estimation for each model is investigated as it is a good representative of estimation accuracy. Finally, the precision regarding the online extraction

of polarization and power curves is inspected to validate the performance of the updated model in the whole operating current range of the PEMFC stack.

Fig. 5 compares the actual measured PEMFC voltage with its estimation by each of the models, including Squadrito, Mann, Amphlett, Srinivasan, and the data fusion method. This comparison has been done for the four previously-discussed experimental DSs. It should be noted that the parameters of all PEMFC models are estimated online by KF and in case of data fusion approach, which fuses the capabilities of the four methods, CI algorithm is used for the

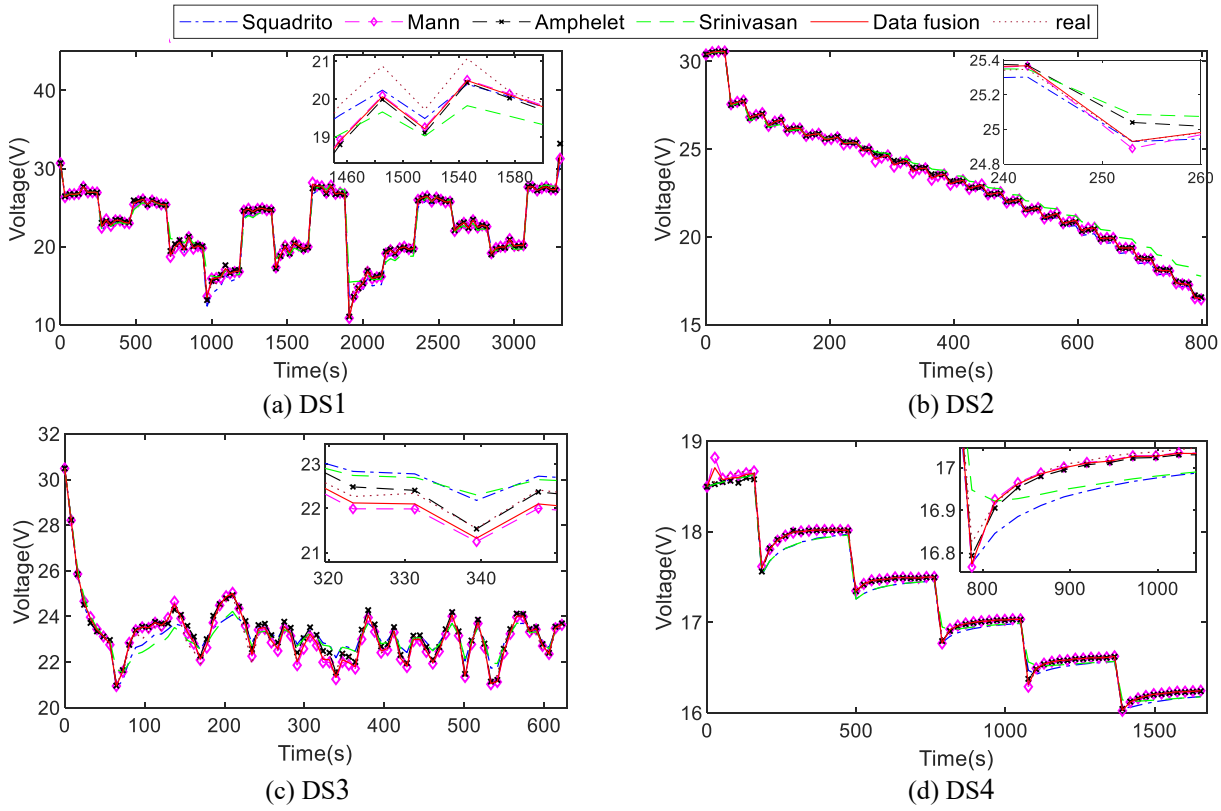

Figure 5: FC voltage estimation by the semi-empirical models and the proposed data fusion.

estimation process. Although this is a good general representation concerning the estimation performance, one cannot draw a firm conclusion on the accuracy of the methods by solely this figure. Therefore, the MSE of the predicted output voltage of the FC has been calculated for all the cases and reported in Table 4. These results demonstrate that the MSE of the Mann and Amphlett models are less than Squadrito and Srinivasan ones. Yet, the proposed data fusion method gives the least MSE among all the studied cases. It is clear that the MSE has been decreased between 7% for DS1 and 20.4% for DS2. The MSE of the other two DSs, DS3 and DS4, have been plummeted by 13.3% and 12.3%, respectively.

Table 4: MSE of identification

	Model	Squadrito	Mann	Amphlett	Srinivasan	Data Fusion
	Algorithm	KF	KF	KF	KF	CI
MSE	DS1($\times 10^{-1}$)	5.00	1.74	1.82	8.07	1.62
	DS2($\times 10^{-2}$)	1.82	0.88	0.99	24.1	0.70
	DS3($\times 10^{-2}$)	15.9	4.28	6.59	18.2	3.71
	DS4($\times 10^{-3}$)	6.25	2.29	2.20	6.34	1.93

The next analysis is about the variance of estimation for each of the utilized models as illustrated in Fig. 6. From this figure, it can be stated that the Srinivasan and Squadrito have the highest variance values which mean that their estimation accuracy is less than the others. When it comes to data fusion results, on one hand, it follows the best prediction provided by the models, as could be deduced from the discussed MSE values. On the other hand, the variance of estimation is also close to the best ones. This behavior implies that data fusion takes advantages of the models' potentials while avoiding their drawbacks.

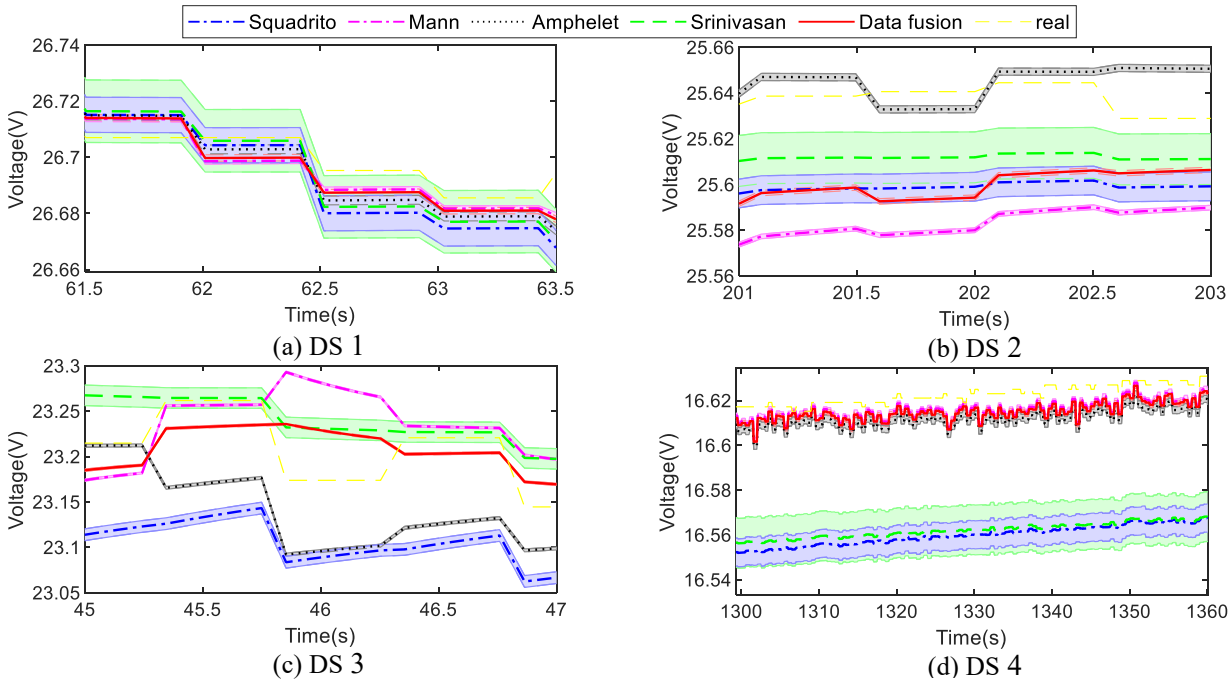

Figure 6: Variance of estimations.

In the last analysis, the capability of the estimation process for online extraction of some important characteristics, namely polarization and power curves, is investigated. These characteristics are normally utilized in the design of online PASs in FCHEVs. It should be noted that since the parameters of all PEMFC semi-empirical models are estimated online by KF, they all show acceptable performance regarding the estimation of the output voltage. This is due to the fact that they try to minimize one single voltage point at each iteration by changing the parameters. However, it is important to check if these models can perform well within the whole operating current range. In this regard, one helpful analysis is to check the estimation of polarization and power curves. Fig. 7 shows the estimation of polarization and power curves for the semi-empirical models and also the fused curves of the data fusion method are depicted in this figure for all DSs. According to this figure, the proposed data fusion method has been able to provide good estimation of voltage and power in all cases. Regarding the other models, it is seen that Amphlett and Mann almost achieve better estimation than Squadrito and Srinivasan. This could be due to the ignorance of considering the temperature and/or mass transport in these two models. To quantitatively highlight the difference among the estimation methods, the MSE of polarization and power curves estimation for each of the discussed cases in Fig. 7 is reported in Table 5. According to this table, the obtained MSE values are in agreement with the discussed points and show the great potential

of the proposed data fusion approach in online characteristics estimation of a PEMFC stack. From Table 5, the put forward method based on data fusion has had the highest estimation accuracy regarding voltage and power curves estimation. Excluding the proposed method from comparison, Amphlett's model has achieved the lowest error in case of DS1 and DS3, Srinivasan's model has reached the minimum error in case of DS2, and Mann's model has had the lowest error in case of DS4. Comparing the data fusion method with the best achieved results, on average, the MSE of data fusion method is 39.64% lower while estimating the polarization curve (19.6% and 15.86% lower than Amphlett's model for DS1 and DS3, 62.5% lower than Srinivasan's model for DS2, and 60.6% lower than Mann's model for DS4) and 36.59% lower while estimating the power curve (29.11% and 54.54% lower than Amphlett's model for DS1 and DS3, 2.43% lower than Srinivasan's model for DS2, and 60.3% lower than Mann's model for DS4).

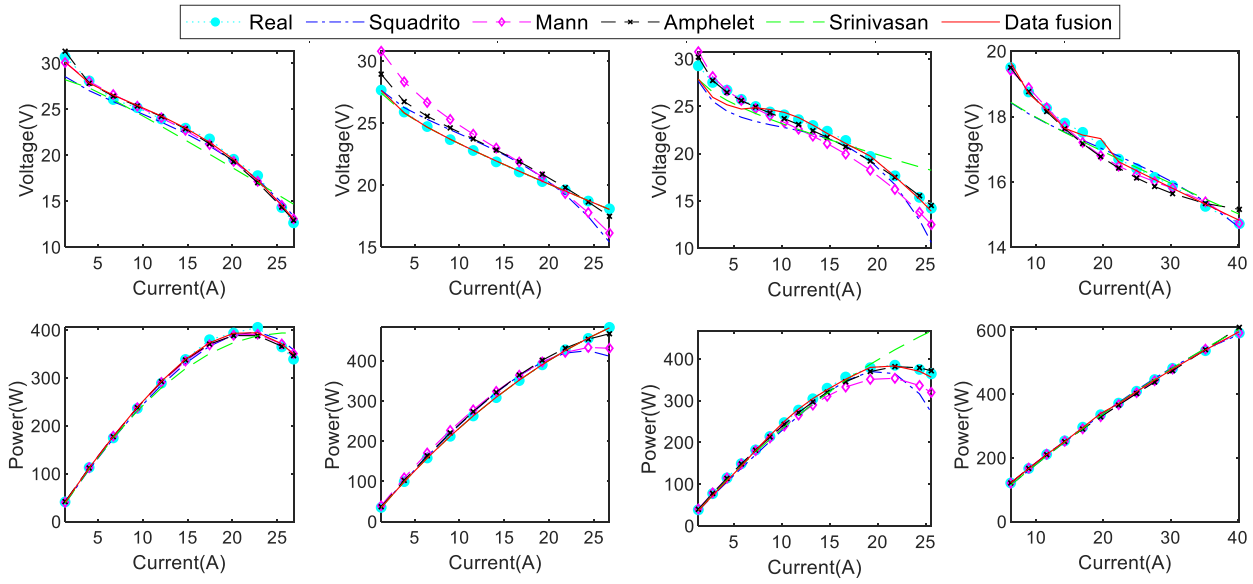

(a) DS 1 (b) DS 2 (c) DS 3 (d) DS 4

Figure 7: Estimation of polarization and power curves for the semi-empirical models and the proposed method based on data fusion.

Table 5: MSE of V-I and P-I curve estimation

	Model	Squadrito	Mann	Amphlett	Srinivasan	Data Fusion
	Algorithm	KF	KF	KF	KF	CI
MSE of V-I	DS1($\times 10^{-1}$)	7.39	1.68	1.53	17.5	1.23
	DS2($\times 10^{-1}$)	11.1	27.9	6.53	0.08	0.03
	DS3($\times 10^{-1}$)	29.3	12.7	6.62	26.2	5.57
	DS4($\times 10^{-2}$)	17.1	2.97	6.49	17.4	1.17
MSE of P-I	DS1($\times 10^{+1}$)	9.02	4.90	4.50	53.3	3.19
	DS2($\times 10^{+1}$)	60.7	40.4	9.17	0.082	0.080
	DS3($\times 10^{+2}$)	8.86	4.04	0.22	12.4	0.10
	DS4($\times 10^{+1}$)	1.94	1.31	5.12	2.98	0.52

6. Conclusion

Estimating the polarization and power curves of a PEMFC stack, as the main source of power in a FCHEV, is highly demanded while designing a PAS. To this end, online parameter estimation methods have become a vital tool for extracting these curves while the system is under operation. This paper proposes an online estimation method based on data fusion to extract the PEMFC characteristics. In this regard, KF is utilized to track the variation of the parameters of four PEMFC semi-empirical models online. Subsequently, a CI algorithm is suggested to estimate the output voltage and the characteristics of the PEMFC stack by fusing the obtained voltage and covariance from each of the PEMFC models. Four different experimental DSs collected from three different 500-W Horizon PEMFCs are utilized to justify the performance of the proposed data fusion approach. The final results illustrate the potential of this suggested method quantitatively as it has achieved the lowest MSE in all the studied cases. Regarding the estimation of polarization and power curves, the MSE of the data fusion method is on average 39.64% and 36.59% lower than other studied approaches. Future endeavors should combine the proposed estimation method of this work with the design of a PAS in a FCHEV to achieve better performance in the management of this vehicle.

CRediT authorship contribution statement

Abolghasem Daeichian: *Conceptualization, Methodology, Software, Formal analysis, Writing - Review & Editing, Supervision*
Razieh Ghaderi: *Methodology, Software, Writing - Original Draft*
Mohsen Kandidayeni: *Formal analysis, Writing - Review & Editing, Resources, Data Curation, Validation*
Mehdi Soleymani: *Writing - Review & Editing, Supervision*
João P. Trovão: *Resources, Data Curation, Funding acquisition, Review, Supervision*
Loïc Boulon: *Resources, Data Curation, Funding acquisition, Review, Supervision*

Declaration of competing interest

The authors declare that they have no known competing financial interests or personal relationships that could have appeared to influence the work reported in this paper.

Acknowledgments

This work was supported in part by the Fonds de Recherche du Québec Nature et Technologies (283370 & 284914), Grant 950e230863 and 950e230672 from Canada Research Chairs Program, and in part by Grant RGPIN-2018-06527 and RGPIN-2017-05924 from the Natural Sciences and Engineering Research Council of Canada. We thank the IEEE VTS Motor Vehicles Challenge 2017 (https://oraprdnt.uqtr.uquebec.ca/pls/public/gscw031?owa_no_site=4656) for providing the open-source file which was used in this manuscript for creating Dataset 3.

References

[1] Wang A, Tu R, Gai Y, Pereira LG, Vaughan J, Posen ID, et al. Capturing uncertainty in emission estimates related to vehicle electrification and implications for metropolitan greenhouse gas emission inventories. Applied Energy. 2020;265:114798.
[2] Chen H, Song Z, Zhao X, Zhang T, Pei P, Liang C. A review of durability test protocols of the proton exchange membrane fuel cells for vehicle. Applied energy. 2018;224:289-99.

[3] Sulaiman N, Hannan M, Mohamed A, Ker PJ, Majlan E, Daud WW. Optimization of energy management system for fuel-cell hybrid electric vehicles: Issues and recommendations. Applied energy. 2018;228:2061-79.
[4] Huang Y, Wang H, Khajepour A, Li B, Ji J, Zhao K, et al. A review of power management strategies and component sizing methods for hybrid vehicles. Renewable and Sustainable Energy Reviews. 2018;96:132-44.
[5] Sulaiman N, Hannan MA, Mohamed A, Ker PJ, Majlan EH, Wan Daud WR. Optimization of energy management system for fuel-cell hybrid electric vehicles: Issues and recommendations. Applied Energy. 2018;228:2061-79.
[6] Zhong D, Lin R, Jiang Z, Zhu Y, Liu D, Cai X, et al. Low temperature durability and consistency analysis of proton exchange membrane fuel cell stack based on comprehensive characterizations. Applied Energy. 2020;264:114626.
[7] Tang W, Lin R, Weng Y, Zhang J, Ma J. The effects of operating temperature on current density distribution and impedance spectroscopy by segmented fuel cell. International Journal of Hydrogen Energy. 2013;38:10985-91.
[8] Wang B, Lin R, Liu D, Xu J, Feng B. Investigation of the effect of humidity at both electrode on the performance of PEMFC using orthogonal test method. International Journal of Hydrogen Energy. 2019;44:13737-43.
[9] Kandidayeni M, Macias A, Boulon L, Kelouwani S. Investigating the impact of ageing and thermal management of a fuel cell system on energy management strategies. Applied Energy. 2020;274:115293.
[10] Song K, Ding Y, Hu X, Xu H, Wang Y, Cao J. Degradation adaptive energy management strategy using fuel cell state-of-health for fuel economy improvement of hybrid electric vehicle. Applied Energy. 2021;285:116413.
[11] Zuo J, Lv H, Zhou D, Xue Q, Jin L, Zhou W, et al. Deep learning based prognostic framework towards proton exchange membrane fuel cell for automotive application. Applied Energy. 2021;281:115937.
[12] Zhou D, Al-Durra A, Matraji I, Ravey A, Gao F. Online energy management strategy of fuel cell hybrid electric vehicles: a fractional-order extremum seeking method. IEEE Transactions on Industrial Electronics. 2018;65:6787-99.
[13] Bizon N. Energy optimization of fuel cell system by using global extremum seeking algorithm. Applied Energy. 2017;206:458-74.
[14] Ettihir K, Boulon L, Agbossou K. Optimization-based energy management strategy for a fuel cell/battery hybrid power system. Applied Energy. 2016;163:142-53.
[15] Ettihir K, Boulon L, Becherif M, Agbossou K, Ramadan H. Online identification of semi-empirical model parameters for PEMFCs. International journal of hydrogen energy. 2014;39:21165-76.
[16] Amamou A, Kandidayeni M, Macias A, Boulon L, Kelouwani S. Efficient model selection for real-time adaptive cold start strategy of a fuel cell system on vehicular applications. International Journal of Hydrogen Energy. 2020;45:19664-75.
[17] Kandidayeni M, Macias A, Amamou A, Boulon L, Kelouwani S, Chaoui H. Overview and benchmark analysis of fuel cell parameters estimation for energy management purposes. Journal of power sources. 2018;380:92-104.
[18] Wang T, Li Q, Qiu Y, Yin L, Liu L, Chen W. Efficiency extreme point tracking strategy based on FFRLS online identification for PEMFC system. IEEE Transactions on Energy Conversion. 2018;34:952-63.
[19] Wang T, Li Q, Yin L, Chen W. Hydrogen consumption minimization method based on the online identification for multi-stack PEMFCs system. International Journal of Hydrogen Energy. 2019;44:5074-81.
[20] Xu L, Li J, Hua J, Li X, Ouyang M. Adaptive supervisory control strategy of a fuel cell/battery-powered city bus. Journal of Power Sources. 2009;194:360-8.
[21] Ettihir K, Cano MH, Boulon L, Agbossou K. Design of an adaptive EMS for fuel cell vehicles. International Journal of Hydrogen Energy. 2017;42:1481-9.
[22] Kandidayeni M, Macias A, Amamou A, Boulon L, Kelouwani S. Comparative analysis of two online identification algorithms in a fuel cell system. Fuel Cells. 2018;18:347-58.
[23] Ghaderi R, Daeichian A. Simultaneously Parameter Identification and Measurement-Noise Covariance estimation of a Proton Exchange Membrane Fuel Cell. 2019 6th International Conference on Control, Instrumentation and Automation (ICCIA): IEEE; 2019. p. 1-5.
[24] Xing Y, Na J, Costa-Castelló R. Real-time adaptive parameter estimation for a polymer electrolyte membrane fuel cell. IEEE Transactions on Industrial Informatics. 2019;15:6048-57.
[25] Mann RF, Amphlett JC, Hooper MA, Jensen HM, Peppley BA, Roberge PR. Development and application of a generalised steady-state electrochemical model for a PEM fuel cell. Journal of power sources. 2000;86:173-80.
[26] Squadrito G, Maggio G, Passalacqua E, Lufrano F, Patti A. An empirical equation for polymer electrolyte fuel cell (PEFC) behaviour. Journal of Applied Electrochemistry. 1999;29:1449-55.
[27] Amphlett JC, Baumert R, Mann RF, Peppley BA, Roberge PR, Harris TJ. Performance modeling of the Ballard Mark IV solid polymer electrolyte fuel cell: II. Empirical model development. Journal of the Electrochemical Society. 1995;142:9.

[28] Srinivasan S, Ticianelli E, Derouin C, Redondo A. Advances in solid polymer electrolyte fuel cell technology with low platinum loading electrodes. Journal of Power Sources. 1988;22:359-75.
[29] Hall D, Llinas J. Multisensor data fusion: CRC press; 2001.
[30] Daeichian A, Honarvar E. Modified covariance intersection for data fusion in distributed nonhomogeneous monitoring systems network. International Journal of Robust and Nonlinear Control. 2018.
[31] Pahon E, Jemei S, Chabriat JP, Hissel D. Impact of the temperature on calendar aging of an open cathode fuel cell stack. Journal of Power Sources. 2021;488:229436.
[32] Strahl S, Costa-Castelló R. Temperature control of open-cathode PEM fuel cells. IFAC-PapersOnLine. 2017;50:11088-93.
[33] H-500 Fuel Cell Stack User Manual. V2.0 ed: Horizon Fuel Cell Technologies; 2010.
[34] H-500 Fuel Cell Stack User Manual. Manual_FCS-C500_V1.1_EN ed: Horizon Fuel Cell Technologies; 2013.
[35] Dayeni MK, Macias A, Depature C, Boulon L, Kelouwani S, Chaoui H. Real-Time Fuzzy Logic Strategy Scheme for Energetic Macroscopic Representation of a Fuel Cell/Battery Vehicle. 2017 IEEE Vehicle Power and Propulsion Conference (VPPC)2017. p. 1-6.